BULLETIN OF THE POLISH ACADEMY OF SCIENCES
TECHNICAL SCIENCES, Vol. 69(5), 2021, Article number: e138815
DOI: 10.24425/bpasts.2021.138815

3D scan contour de-featuring for improved measurement accuracy – a case study for a small turbine guide vane component

Marcin JAMONTT[1] **and Paweł PYRZANOWSKI**[2*]

[1] General Electric Company, al Krakowska 110-114, 02-265 Warsaw, Poland
[2] Institute of Aeronautics and Applied Mechanics, Warsaw University of Technology, ul. Nowowiejska 24, 00-665 Warsaw, Poland

Abstract. 3D scanning measurements are gaining popularity every year. Quick inspections on already captured point clouds are easy to prepare with the use of modern software and machine learning. To achieve repeatability and accuracy, some surface and measurement issues should be considered and resolved before the inspection. Large numbers of manufacturing scans are not intended for manual correction. This article is a case study of a small surface inspection of a turbine guide vane based on 3D scans. Small surface errors cannot be neglected as their incorrect inspection can result in serious faults in the final product. Contour recognition and deletion seem to be a rational method for making a scan inspection with the same level of accuracy as we have now for CMM machines. The main reason why a scan inspection can be difficult is that the CAD source model can be slightly different from the inspected part. Not all details are always included, and small chamfers and blends can be added during the production process, based on manufacturing standards and best practices. This problem does not occur during a CMM (coordinate measuring machine) inspection, but it may occur in a general 3D scanning inspection.

Key words: 3d scan; flatness; turbine guide vane; small surfaces; point clouds; contour recognition; contour de-featuring.

1. INTRODUCTION

Inspection of large surfaces on a large component based on 3d scanning has been the focus of extensive research over recent years. Cuypers [1] highlights that 3D scanners have a wider inspection area range than conventional CMM machines and, therefore, they are the only desired method for that kind of inspection. It is crucial for big components, machines, and assembled groups of mechanical parts, especially when inspected in working conditions.

The situation is different if the inspected component can be inspected with both methods and assurance that the results are identical is desired. CMM is a method that has standardized ISO requirements [2] and practices for every kind of inspection, and whose results are fully reliable and repeatable under the same measuring conditions.

3D scanning inspection is not a new field, but this method is still not standardized enough to provide reliable results. Many deviations may occur during scan capture, like unregistered or partially registered surfaces, blurs, holes, or additional background noise [3].

The case study presented in this article describes an inspection performed on a turbine guide vane component, which was pre-machined to identify datum planes for further operations. Such a manufacturing situation is crucial to prevent huge deviations. Proper inspection is of fundamental importance not only for part acceptance but also for the qualification of the overall manufacturing process. Turbine guide vanes play an important role in turbine engines. Their overall shape comprises a lot of complicated and relatively small surfaces or areas with restrictive aerodynamic requirements. Therefore, inaccuracies or misses in inspection can significantly affect the overall engine efficiency and even lead to failure.

Dedicated software like GOM Inspect [4] or Geomagic Control X [5] can handle a lot of issues related to 3D scanning imperfections, but there are still some areas for improvement. Based on scan and CMM comparisons, this study has identified the main issues related to the 3D scanning process, especially for relatively small surfaces of the measured part.

2. CASE STUDY – SURFACE FLATNESS INSPECTION

In this research, a single airfoil vane with a machined surface located on the front of the inner band was used (Fig. 1). This component is less than 200 mm of the overall width. The area of interest can be described as a rectangle with ~ 5 mm width and ~ 80 mm height. The goal is to inspect the flatness of the surface [6, 7] as a reference datum for further operations. This surface needs to be precisely machined with the overall flatness of 0.1 mm tolerance zone (Fig. 2).

Inspection on CMM is relatively easy as only a simple path for scanning with a CMM probe needs to be defined. In this case, two bridged scanning lines with 205 measuring points to take measurements at were defined (Fig. 3). All those points are used to define two parallel datums with the smallest distance which can be used to include all points within them. The results

*e-mail: pyrzan@meil.pw.edu.pl

Manuscript submitted 2021-04-07, revised 2021-06-15, initially accepted for publication 2021-07-28, published in October 2021

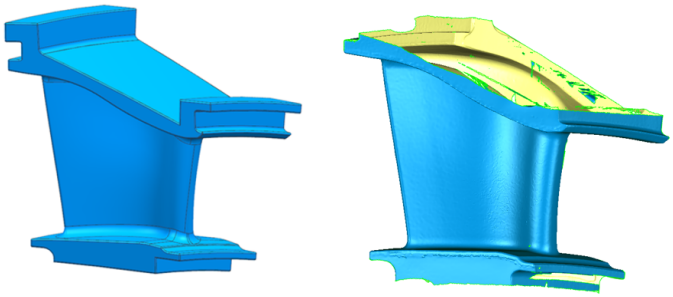

Fig. 1. Small turbine guide vane example – overall part shape example/scan example

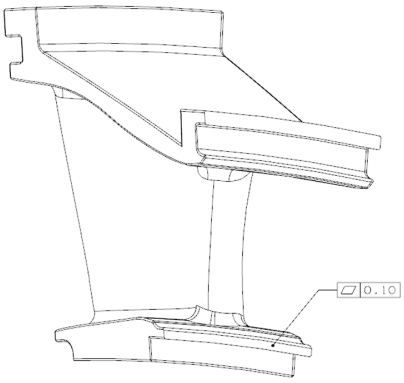

Fig. 2. Specification requirement, the flatness of the small surface. Point of interest for this research

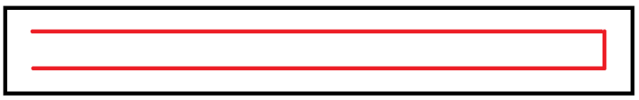

Fig. 3. Flatness measurement plan for CMM – 2 scanning lines, 205 points

of the measurements performed are presented in Fig. 4. The inspection was performed with additional filtering of the points, called "unusual filtering", which entails removing all points that are located too far from other points in the group (Fig. 5). This is a typical solution for small surfaces used to eliminate errors (vibrations, local blurs, or micro-holes). There are many methods to choose how many of these points need to be removed. The most popular are Gauss filters and 1/2/3 sigma criterium (68.3%/95.5%/99.7%). These parameters should be clearly de-

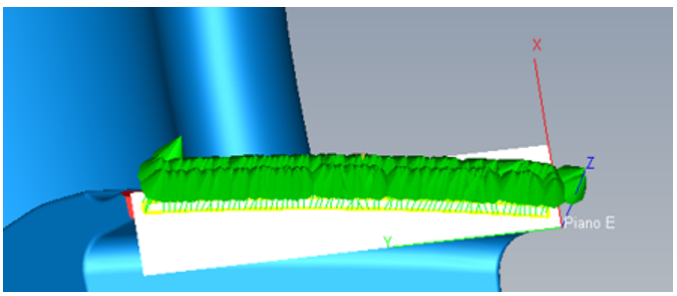

Fig. 4. CMM points for flatness calculations

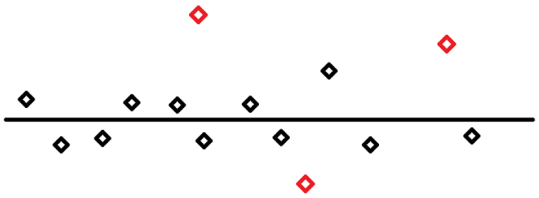

Fig. 5. CMM unusual filter for measured points

fined by an experienced operator with the correlation of production method stability.

Results for 15 components were collected, and it was noticed that all the measured deviations of flatness were within an acceptable divergence, and only three exceeded that deviation. All the results are presented in Table 2 at the end of this article. CMM used Zeiss Accura II with Vast XT and Vast XXT probe heads, Calypso 2020 software with curve and freeform modules.

It is desired to achieve the same accuracy and match with 3D scans to allow this kind of inspection to be equivalent to and interchangeable with CMM. The future of 3D scan verification lies with its repeatability and automation. A massive collection of scans can be inspected, and automated scripts used to compare them all are based on the same assumptions. Although the scanning process itself may be time-consuming, the inspection can be done physically once only and then repeated automatically by well-written scripts or macros.

A 3D scan inspection was performed for the same 15 vanes set using GOM ATOS Core 3D Blue Light with an accuracy of 0.019 mm. The results were not reliable at the beginning, as all measured values were up to twice as high as CMM measurements. That was a starting point for this article study – how to solve this issue and assure the reliability of an automatic inspection.

2.1. Contour as a culprit of measuring error

To identify the problem, a comparison of the positioned point cloud related to the original CAD model was used. It was noticed that the CAD model had no blend present in the area of interest (Fig. 6.), whilst the real parts captured by a scan had this feature. It is not obvious to any automatic tool whether the points on the blend should be filtered (and where to start to identify this feature) or if it is still part of the area of the flat surface, but with too high deviation. In this case, the Geomagic Control X tool used some points from the blend area (Fig. 7) to calculate the overall flatness of this surface. This was the reason for the increased deviation. From the perspective of assessing one component, such deviations can be easily noticed and eliminated. But if $\sim$ 100 similar surface requirements exist on the part undergoing inspection, then repeating it on a full set which can include $\sim$ 100 parts in total can be a serious issue. It is advisable to prepare a repair plan for this measurement and use AI to prepare a report for all parts automatically. A natural need arises to improve it without a manual scan by scan optimization, and without the need to investigate the occurrence of the issue, no matter how intelligent the scripts put inside the software and measurement plan are.

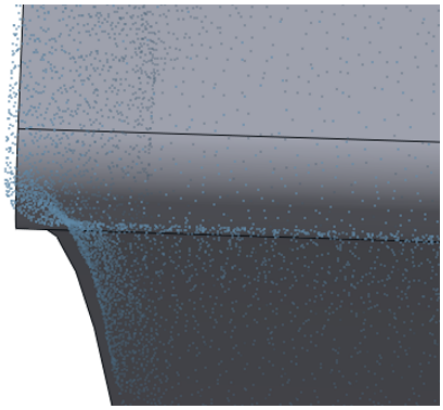

Fig. 6. Point Cloud vs CAD surfaces comparison: a region of curvature exists only on the scan

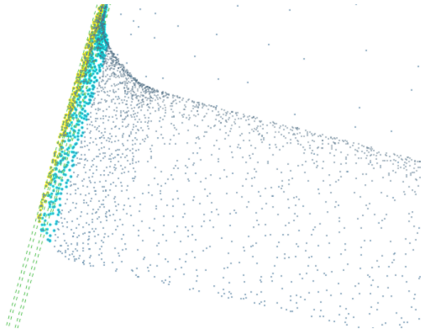

Fig. 7. Automatically selected points for flatness measurements in Geomagic Control X

2.2. 3D Scan and CMM comparison – what can be learned from touch technology?

A correctly performed CMM inspection was done on the predefined safety regions on part features. This means that the whole surface is not measured, but a boundary area is defined to prevent all worst-case scenarios of possible part deviations and to avoid the areas containing blends or chamfers which may or may not exist on a part. A decreased surface area is measured within the defined boundary (Fig. 8) to prevent the occurrence of the mentioned unpredictable phenomena. This research aims to introduce a similar method for a 3D scan, in which a scan would be de-featured before inspection (Fig. 9).

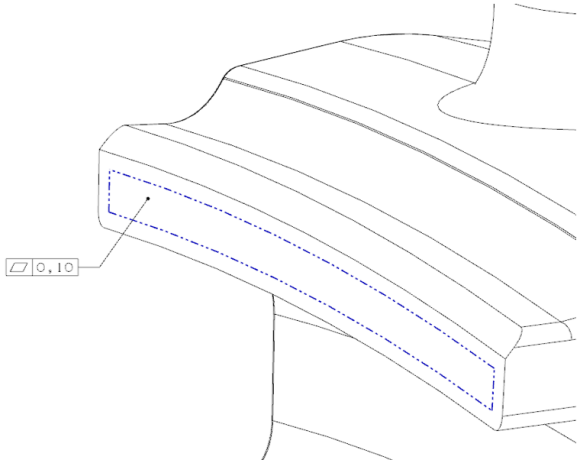

Fig. 8. The boundary of the CMM scanning area

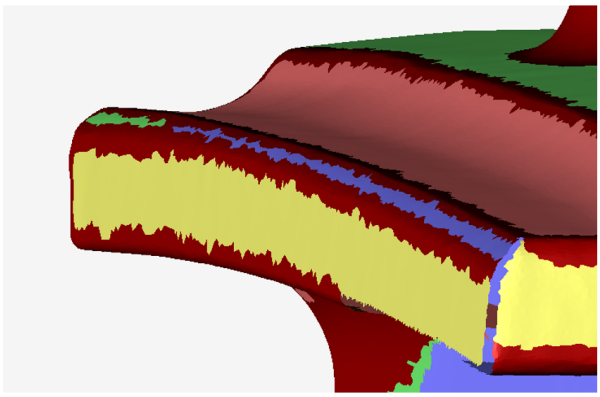

Fig. 9. Red colour – filtered triangles for contour detections based on the 3D mesh. All other colours represent different surfaces and have no additional meaning

3. 3D SCAN DATA PROCESSING

3.1. Handling point cloud data

There are many algorithms and approaches available and utilized by researchers. Fan [8] documented an approach for extracting curve profiles from 3D scan point clouds. Lingxiao [9] developed a method for fitting primitives (plane, cylinder, circle, etc.) on a noisy point cloud. Liu [10] studied grouping regions of points to identify the same kinds of surfaces, even more sophisticated than simple primitives. Yang [11] developed an improved algorithm for feature extraction on a large volume scan, which was also previously studied by Zhong [12] or Pauly [13]. Complicated object detection can also be used to segment features from photos, a method which was studied by Fehr [14]. Hackel [15] took a very noisy and complicated mesh of a building complex to deconstruct its overall contours. The result is extraordinary, showing how powerful modern algorithms can be. Artificial Intelligence can easily learn even complex object shapes from the point cloud to enable finding them on the next data set [16].

Similar solutions are available in Geomagic Design X [17] or Geomagic Wrap [18], commercial reverse engineering software. It is advisable to use only one type of software, as such an approach is cheaper, faster, and easier to automate. This research was done with the use of Geomagic Control X – software dedicated only for inspection (GOM Inspect as an alternative).

For this study, it was not necessary to follow such complicated algorithms as used by the authors above. The aim was to adhere to simple trigonometric relationships, as a scan is a big set of triangles which are easy to compare using well-known math equations.

3.2. Computing mesh data

A 3D scan point cloud is usually triangulated into a mesh structure, which can be utilized in the segmentation of the mesh data [19]. Lavoue [20] presented an original method to decom-

pose 3D mesh with contour recognition. Centin [21] added a solution to filter spikes, reversed/crossing triangles (duplicated), and non-manifolds (triangles connected to a mesh with only one point or edge). It is impossible to draw straight border lines on a scan the way it can be done on regular CAD models, so segmentation should be performed near the theoretical changes of curvature. This would be the starting point.

4. CASE STUDY – SURFACE FLATNESS INSPECTION

4.1. Manual correction

Modification necessary to overlay a scan over a CAD model can be done manually:

- Mesh manual update – the mesh can be cleaned manually to remove contours; this is very time-consuming, imprecise, and needs to be performed one by one on all the scans.
- Best fit to the measured surface –this can work for flatness, but it is a solution only for a specific face. For the whole part ($\sim$ 100 surfaces to inspect), it will not be an efficient process for iteration with every surface. The real-world requirements for a profile of a surface in relation to a specific datum system do not allow the implementation of this solution.

Based on the above, it is justified to implement an automated solution for a mass inspection set.

4.2. Contours defeaturing

In contrast to the researchers quoted in this chapter [22–26], this study has developed a simple algorithm with very basic math calculations. The main reason is very simple – practical use on a big batch of 3D scans with a very quick response. The tool developed here can calculate a real 3D scan for the described turbine guide vane in about 2 minutes [27]. This is the time needed to go through 2 million points in a typical top-quality 3D scan. For a full set of scans (around 50), it takes less than 2 hours to complete.

The only disadvantage of this approach is that the theoretical radial value (1 mm – specified by a casting process to avoid sharp edges) is not exact, and it is impacted by small errors dependent on the scan quality and point density. Yet, in the approach presented herein, this has a marginal impact and the average value (calculated based on all triangles from the chosen edge) is almost equal to the theoretical one (1 mm), and the sample standard deviation is 0.6 (Table 1). If radial values smaller than 2 mm were removed, it would be possible to filter off all the deviations (triangles outside the flat surface).

A course of action prescribed by Di Angelo [22,23] was used for finding fillets and chamfers on scanned surfaces. Li [24] introduced and improved Harris' algorithm for feature extraction. Based on those three works, a C# script was used to filter points which are located on a contour curvature shape. In contrast to the authors mentioned above, the goal was not to find so many examples of curvature and highlight them in a report, but merely to filter points not lying on a local planar surface, or a high intended component specification curvature.

Table 1
Calculated radius values for deleted triangles

R (theoretical exact) [mm]	R (average for all pairs) [mm]	Median	Sample Standard Deviation	Number of triangle pairs
1.0	0.971836	0.822039	0.607124	4771

The first step is to group all triangles with common points (Fig. 10). Applying this criterion only, triangles will be repeated in many groups if they are distributed around a unique point. The final script can be slower if all the criteria are kept, but it will be much easier to code. Modern computers are very fast, and this approach will not impact their performance too much [27]. There are many AI scripts available, like a k-nearest neighbour or homogenous neighbour [24] to create and sort those groups, but in this study very simple and fast algorithms like C#: list.Sort() will be used.

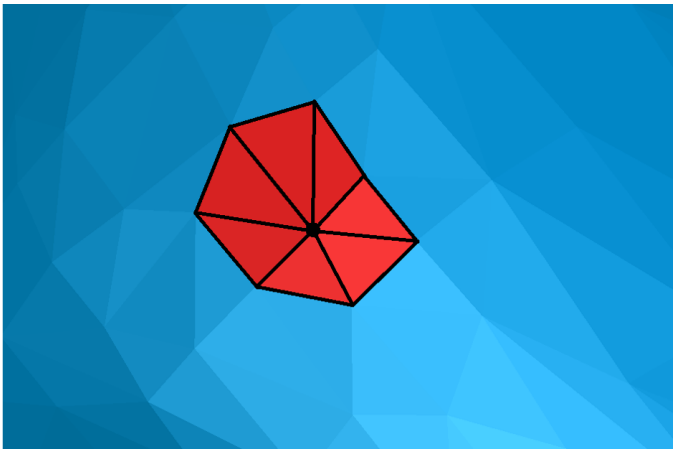

Fig. 10. A group of triangles with a common point

An example of groups of flat and curved geometries is presented in Fig. 11. This approach can be extended to cover a chord height (for the circle described on the triangle) of overall groups, a scenario included in the work of Tao [25]. Very sophisticated examples are also included in the work of Palma [26]. A simpler solution is used by Jagannathan [28] to define a curvedness index. In the approach adopted in this study, it will also be much simpler.

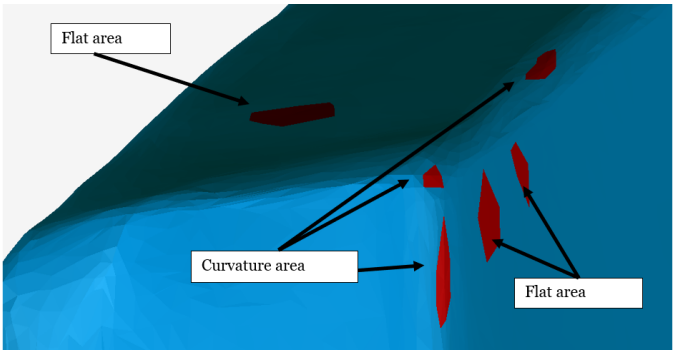

Fig. 11. Region of triangles on a 3D scan

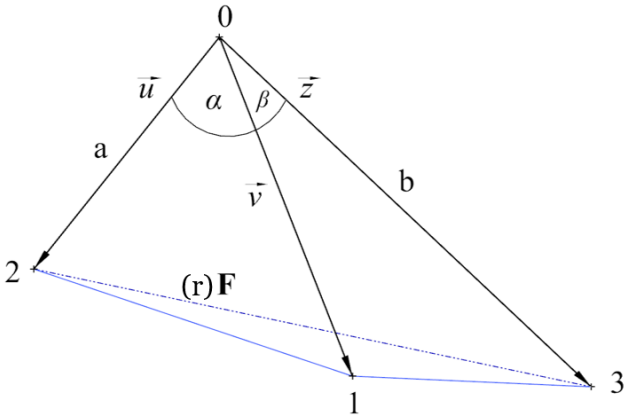

Fig. 12. Region of triangles on a 3D scan. "F" reaches a theoretical maximum if triangles lie on the same plane. The sum of $\alpha+\beta$ defines a θ total angle. Points 0 and 1 are common for both triangles

A decision to define a variable – "F" – flatness indicator for all triangle pairs in a group was made (Fig. 12). To calculate a 2D "F" value, a formula can be used for calculating an angle between two vectors and then a cosine rule:

$$\theta = \alpha + \beta = \arccos\left(\frac{\vec{u} * \vec{v}}{\|\vec{u}\|\,\|\vec{v}\|}\right) + \arccos\left(\frac{\vec{v} * \vec{z}}{\|\vec{v}\|\,\|\vec{z}\|}\right), \quad (1)$$

$$F = \sqrt{a^2 + b^2 - 2ab * \cos\theta}\,. \quad (2)$$

If "rF" (real F value – measured between points 2 and 3 in 3D) and "F" are equal, it means that the pair of triangles lie on a perfectly flat part of the surface. If "rF" is smaller than "F", it means that the triangles lie in a region of curvature – a 3D relation will always be smaller (Fig. 13).

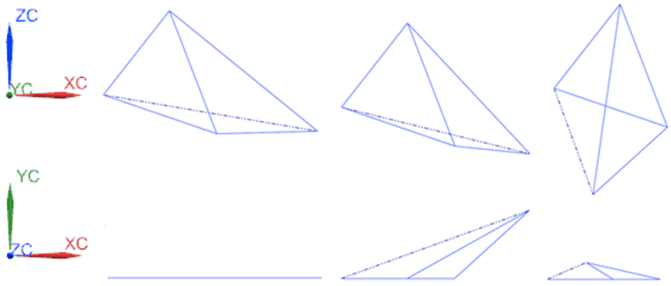

Fig. 13. Flatness checking for a pair of triangles. "rF" length varies with curvature change, "rF" in 3D is always smaller than "F". A visualization on two planes – ZY (above) and XY (below). "rF" is presented as a dashed line

If a criterion that "rF" varies between 0F-1F is introduced, a universal criterion for flatness can be created (Fig. 14). A perfect flatness would have $rF/F = 1$. The smaller the value calculated, the more noise in the point cloud. A new constant "cF" just needs to be defined here (curvature flatness check as a constant ratio for every pair of triangles). A cF value used in this research was set at 0.998. This value was set based on scan

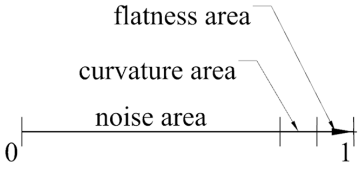

Fig. 14. Defining a "cF" constant value within an "F" variable. $x = cF = rF/F$ where 1 is the maximum value possible. The exact value for noise/curvature/flatness border is not constant, so it needs to be determined based on a particular scenario and/or a component

quality and overall batch sample and may vary for a different part. It is rather a cosmetic filter, not a permanent value.

$$cF = rF/F, \quad (3)$$

$$cF \in \langle 0;1\rangle \iff 0 \le cF \le 1. \quad (4)$$

4.3. Defining a local radius

When all triangle pairs are grouped, it is necessary to introduce an additional filter to verify the radius value. As it is advisable to keep all the intended curvatures, only elimination of small features is required. To calculate a radius, a universal formula for a circle circumscribed about a triangle can be used (Fig. 15):

$$R = \frac{f_1 * f_2 * rF}{4P}\,. \quad (5)$$

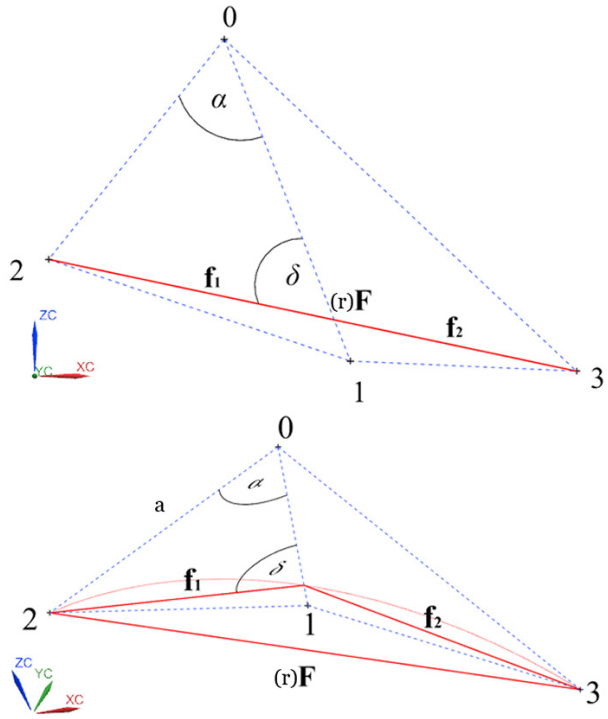

Fig. 15. Calculating the "R" value based on some universal math formulas. The picture at the top – a 2D projection, the picture at the bottom – a 3D isometric view. The lines in red define the calculated 3D triangle. F = f1 + f2

To calculate P – triangle total area, Heron's formula can be implemented:

$$P = \sqrt{\frac{(f_1+f_2+rF)*(f_1+f_2-rF)*(f_1-f_2+rF)*(-f_1+f_2+rF)}{16}}. \quad (6)$$

And finally, for $f1$ (trigonometric functions – sine rule) and $f2$ ($F = f1 + f2$):

$$f_1 = \frac{a * \sin\delta}{\sin\alpha}, \quad (7)$$

$$f_2 = F - f_1. \quad (8)$$

Based on these, it is possible to calculate the "R" radiuses defined by all triangle pairs given. Unfortunately, it is still not enough to check the real values on 3D point clouds; it is necessary to add one last aspect to this approach to do so.

4.4. Scan resolution and ellipse adjustment

The radius calculated for a 2D ideal scenario (perpendicular to the blend surface) will not be the same as that represented inside a real 3D space. Triangles are randomly spread on the blend surface and the calculated radius needs to include ellipse transformation (Fig. 16). To adjust for this phenomenon, the scan resolution and real manufacturing experience could be included to achieve the desired blend size. If the smallest intended radius is equal to 5 mm and it is known that manufactured blends can achieve a maximum of 1 mm, an additional factor can be added here, such as the fact that the enlarged radius of an ellipse can be twice as big. In this approach a factor of EE (ellipse enlargement) = 1.6 will be used. To filter all radii from the 3D scan, all the calculated triangle pairs with radii smaller than 1.6 mm will be removed. For a good quality scan, there will be more triangles on a curved surface, which should not affect this increase too much. In other words, a typical increment should vary by around 0.4∼1.6 (based on a 0.6 sample standard deviation – Table 1). The more triangles inside a closed surface, the less noise there is and the more the shape of the ellipse approximates a real circle. Commercial software uses a big amount of data to calculate the exact radius value, and this is usually an average value calculated for thousands of points, which is similar to the results obtained in this study. This adjustment for an ellipse error provides sufficient justification for filtering the data on a micro-level.

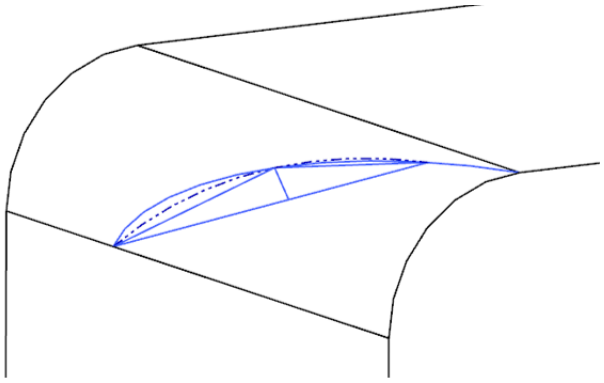

Fig. 16. The calculated radius on the real scan triangles is circumscribed about an ellipse. An additional factor must be used to take this phenomenon into account. A solid line – ellipse – a cross-section through the real surface; dashed line – circle, slightly deviated from a real surface

4.5. Final script

The coded script inspects all triangles by groups spread around the same point. Every group contains n pairs of triangles which can be checked separately. 3 variables are used: the flatness condition, the radius of curvature, and an enlargement factor for a 3D ellipse. To pass the test all the pairs need to be within the accepted range. Only one failure is enough to delete a particular group from the file. In the end, the script saves a simplified file, and a new measurement can be performed on the test components. The full algorithm is presented in Fig. 17.

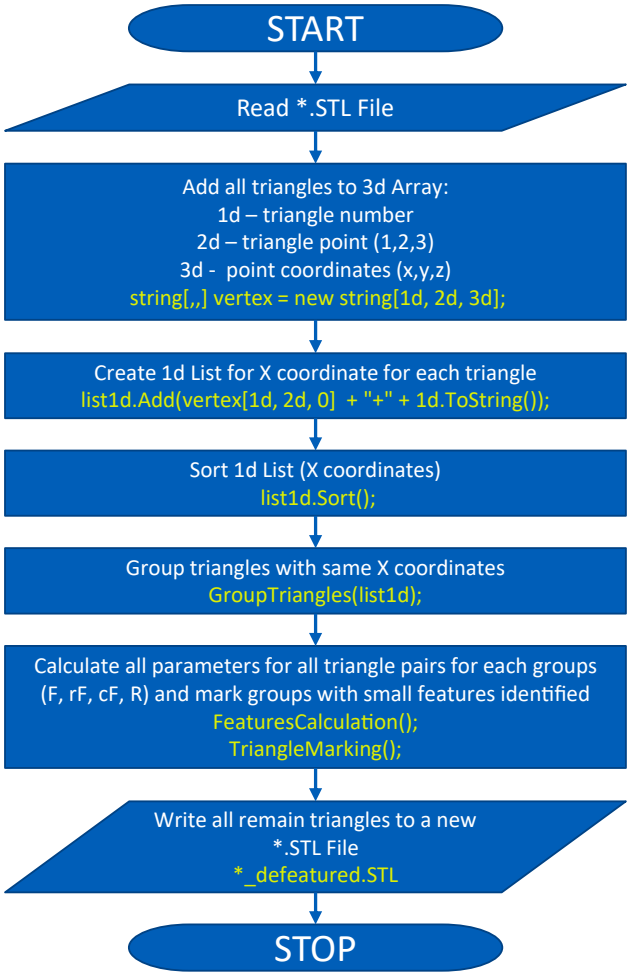

Fig. 17. Schema of our algorithm for scan data filtering

The main potential deviation scenarios are presented in Fig. 18. Chamfer features can be identified with this script as a regular blend in the area of angle change. A simplified defeatured file created by this algorithm is presented in Fig. 19. An additional benefit of this script is that there is also a picture of additional surface issues like blurs or local waviness, which is also removed from the final inspection file.

Type of features	blend	chamfer
To be deleted	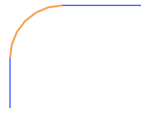	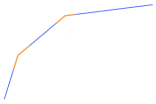
	$R = 1$ mm	1×1 mm
Type of features	Intended design blend	Airfoil curvature
To maintain	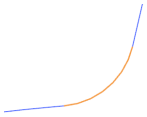	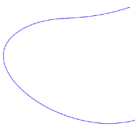
	$R > 15$ mm	$R > 100$ mm

Fig. 18. The basic design features to identify during de-featuring

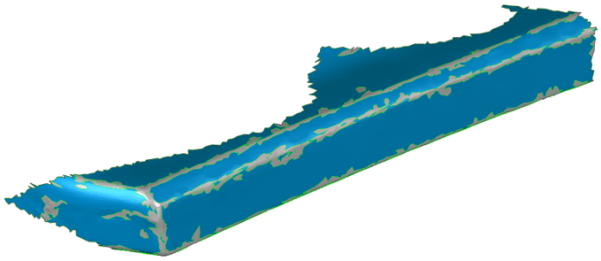

Fig. 19. Example of de-featured surface (some surface defect affected)

5. RESULTS AND VERIFICATIONS

As, for now, comparable measurements for CMM and original 3D scans have been obtained, scan contour de-featuring and new measurement inspection with automated scripts (Table 2) can be performed. De-featured surfaces are easier to inspect, and the results are satisfactory and comparable to a CMM inspection. All the new measurements have similar values when compared to a CMM inspection, which justifies this approach. The following interesting conclusions can be drawn:

A 3D scanning inspection of a raw scan can reveal unreliable data and can cause more part rejection/repair demands than are really needed. This study shows that CMM captured 3 parts out of tolerance, de-featured scans captured 4 (one part is very close to the tolerance limit value on both methods) parts out of tolerance, while raw scans resulted in 9. It is 300% as high and proves that 3D scanning inspections should include additional requirements for quality and credibility.

Not every scan needs simplification, as some of them already have missing faces, or the software inspection tools captured the right range of points. As a potential check of legitimacy for de-featuring can take the same amount of time, it is still justifiable to run it on all files.

All de-featured scans have higher tolerance value ranges – this is simple to explain as a scan inspection has ~ 50 times more points ($\sim$2500–5000) to calculate than a CMM set ($\sim$100–200). It can be underlined as a potential benefit of the 3D scanning method that the measurement plan has a higher range for surfaces, especially small ones. Hardware accuracy can be neglected, as it does not affect the values on an observable level.

Table 2

Flatness Measurement result comparison for a set of vanes (CMM accuracy: 0.0012 mm, 3D Scan accuracy: 0.019 mm)

Measured Vane	CMM Flatness	Flatness measured on raw 3D scan	Difference [3d scan vs CMM]	Flatness measured on a scan with removed contours	Difference [3D scan vs CMM]
1	0.070	0.077	9.09%	0.076	7.89%
2	0.069	**0.149**	53.69%	0.074	6.76%
3	0.066	**0.132**	50.00%	0.069	4.35%
4	0.098	**0.132**	25.76%	**0.108**	9.26%
5	**0.109**	**0.136**	19.85%	**0.132**	17.42%
6	**0.103**	**0.145**	28.97%	**0.111**	7.21%
7	0.079	0.084	5.95%	0.082	3.66%
8	0.082	0.094	12.77%	0.083	1.20%
9	**0.105**	**0.159**	33.96%	**0.113**	7.08%
10	0.068	0.073	6.85%	0.069	1.45%
11	0.070	0.078	10.26%	0.071	1.41%
12	0.062	0.065	4.62%	0.065	4.62%
13	0.051	**0.106**	51.89%	0.055	7.27%
14	0.078	**0.153**	49.02%	0.079	1.27%
15	0.079	**0.115**	31.30%	0.083	4.82%

6. DISCUSSION AND CONCLUSIONS

Precise measurement is very crucial for manufactured parts, and 3D scans still have a lot of potential critical issues to discover and solve within new algorithms. This study shows great potential for these kinds of measuring strategies in the modern world, highlighting major threats which need to be taken into consideration. The approach to contour limitation taken here can be used for all scans and with different filtering criteria. The authors truly believe that in the future these kinds of functions will be also available in commercial software.

The presented method is quite fast (less than five minutes for 0.5–2 million triangles) which is comparable to the other different functions available in commercial software for 3D scan data management. The main advantage is the simplicity of the algorithm ($\sim$ 1000 code lines), which can be easily followed and even simplified by other researchers. Precision is not high for the small groups of triangles (standard deviation 0.6 mm for a small 1 mm blend), but the average value calculated from the entire blend surface is almost equal to the nominal (Table 1). This cannot be treated as a disadvantage, as the commercial software also needs a bigger set of data for a reliable result. Our method is proving that the proper data filtering can give comparable results with the traditional CMM method.

CMM method is still more popular, as the simplified stable production lot can be inspected one by one very fast. The main benefit of the 3D scan is that we can see the overall part shape and inspect as many features as we want, even in the future, when the part is already in the engine. A much bigger set of data (measured points) for the same surface is also an important benefit for the 3D scan technique.

The subject of this article, a turbine guide vane, is relatively small, but it must be taken into account that aircraft engines have much smaller components than heavy-duty machines. It is crucial to develop a proper inspection method for such parts if the industrial demand is to supersede CMM machines or make them exchangeable.

ACKNOWLEDGEMENTS

This work has been supported by the Joint Venture agreement between GE Company Poland and Warsaw University of Technology.

REFERENCES

[1] W. Cuypers, N. Van Gestel, A. Voet, J. P. Kruth, J. Mingneau, and P. Bleys, "Optical measurement techniques for mobile and large-scale dimensional metrology," *Opt. Lasers Eng.*, vol. 47, no. 3–4, pp. 292–300, 2009, doi: 10.1016/j.optlaseng.2008.03.013.

[2] An International Standard: Geometrical product specifications (GPS) – Acceptance and reverification tests for coordinate measuring machines (CMM), ISO 10360:2011, 2011.

[3] B.S. Marció, P. Nienhaysen, D. Habor, and R.C.C. Flesch, "Quality assessment and deviation analysis of three-dimensional geometrical characterization of a metal pipeline by pulse-echo ultrasonic and laser scanning techniques," *Meas. J. Int. Meas. Confed.*, vol. 145, pp. 30–37, 2019, doi: 10.1016/j.measurement.2019.05.084.

[4] GOM Inspect Brochure, 2019. [Online]. Available: https://www.3dteam.pl/wp-content/uploads/2020/11/GOM-Software.pdf.

[5] Geomagic Control X Overview, 2020. [Online]. Available: https://www.3dsystems.com/sites/default/files/2020-10/3d-systems-controlx-en-letter-web-2020-10-07.pdf.

[6] An International Standard: Dimensioning and Tolerancing, ASME Y14.5, 2019.

[7] An International Standard: Geometrical tolerancing, ISO 1101, 2017.

[8] J. Fan, L. Ma, A. Sun, and Z. Zou, "An approach for extracting curve profiles based on scanned point cloud," *Meas. J. Int. Meas. Confed.*, vol. 149, p. 107023, 2020, doi: 10.1016/j.measurement.2019.107023.

[9] L. Li, M. Sung, A. Dubrovina, L. Yi, and L. J. Guibas, "Supervised fitting of geometric primitives to 3D point clouds," *Proc. IEEE Comput. Soc. Conf. Comput. Vis. Pattern Recognit.*, 2019, pp. 2647–2655, doi: 10.1109/CVPR.2019.00276.

[10] Y. Liu and Y. Xiong, "Automatic segmentation of unorganized noisy point clouds based on the Gaussian map," *CAD Comput. Aided Des.*, vol. 40, no. 5, pp. 576–594, 2008, doi: 10.1016/j.cad.2008.02.004.

[11] Y. Yang, H. Fang, Y. Fang, and S. Shi, "Three-dimensional point cloud data subtle feature extraction algorithm for laser scanning measurement of large-scale irregular surface in reverse engineering," *Meas. J. Int. Meas. Confed.*, vol. 151, p. 107220, 2020, doi: 10.1016/j.measurement.2019.107220.

[12] Y. Zhong, "Intrinsic shape signatures: A shape descriptor for 3D object recognition," *2009 IEEE 12th Int. Conf. Comput. Vis. Work. ICCV Work,* 2009, pp. 689–696, 2009, doi: 10.1109/ICCVW.2009.5457637.

[13] M. Pauly, R. Keiser, and M. Gross, "Multi-scale Feature Extraction on Point-Sampled Surfaces," vol. 22, no. 3, pp. 281–289, 2003.

[14] D. Fehr, W.J. Beksi, D. Zermas, and N. Papanikolopoulos, "Covariance based point cloud descriptors for object detection and recognition," *Comput. Vis. Image Underst.*, vol. 142, pp. 80–93, 2016, doi: 10.1016/j.cviu.2015.06.008.

[15] T. Hackel, J.D. Wegner, and K. Schindler, "Contour detection in unstructured 3D point clouds," *Proc. IEEE Comput. Soc. Conf. Comput. Vis. Pattern Recognit.*, 2016, pp. 1610–1618, doi: 10.1109/CVPR.2016.178.

[16] H. Wang, C. Wang, H. Luo, P. Li, Y. Chen, and J. Li, "3-D Point Cloud Object Detection Based on Supervoxel Neighborhood With Hough Forest Framework," *IEEE J. Sel. Top. Appl. Earth Obs. Remote Sens.*, vol. 8, no. 4, pp. 1570–1581, 2015, doi: 10.1109/JSTARS.2015.2394803.

[17] Geomagic Design X Overview, 2020. [Online]. Available: https://www.3dsystems.com/sites/default/files/2019-11/3d-systems-designx-en-letter-web-2019-10-25.pdf.

[18] Geomagic Wrap Overview, 2020. [Online]. Available: https://www.3dsystems.com/sites/default/files/2019-11/3d-systems-wrap-en-letter-web-2019-11-01.pdf.

[19] The StL Format, 2021. [Online]. Available: http://www.fabbers.com/tech/STL_Format.

[20] G. Lavoué, F. Dupont, and A. Baskurt, "A new CAD mesh segmentation method, based on curvature tensor analysis," *CAD Comput. Aided Des.*, vol. 37, no. 10, pp. 975–987, 2005, doi: 10.1016/j.cad.2004.09.001.

[21] M. Centin and A. Signoroni, "RameshCleaner: conservative fixing of triangular meshes," *STAG Smart Tools Apps Graph. – Eurographics Italian Chapter Conference*, 2015, doi: 10.2312/stag.20151300.

[22] L. Di Angelo, P. Di Stefano, and A. E. Morabito, "Fillets, rounds, grooves and sharp edges segmentation from 3D scanned surfaces," *CAD Comput. Aided Des.*, vol. 110, pp. 78–91, 2019, doi: 10.1016/j.cad.2019.01.003.

[23] L. Di Angelo and P. Di Stefano, "Geometric segmentation of 3D scanned surfaces," *CAD Comput. Aided Des.*, vol. 62, pp. 44–56, 2015, doi: 10.1016/j.cad.2014.09.006.

[24] Q. Li, X. Huang, S. Li, and Z. Deng, "Feature extraction from point clouds for rigid aircraft part inspection using an improved Harris algorithm," *Meas. Sci. Technol.*, vol. 29, no. 11, 2018, doi: 10.1088/1361-6501/aadff6.

[25] Y. Tao, Y. Q. Wang, H. B. Liu, and M. Li, "On-line three-dimensional point cloud data extraction method for scan-tracking measurement of irregular surface using bi-Akima spline," *Meas. J. Int. Meas. Confed.*, vol. 92, pp. 382–390, 2016, doi: 10.1016/j.measurement.2016.06.008.

[26] G. Palma, P. Cignoni, T. Boubekeur, and R. Scopigno, "Detection of Geometric Temporal Changes in Point Clouds," *Comput. Graph. Forum*, vol. 35, no. 6, pp. 33–45, 2016, doi: 10.1111/cgf.12730.

[27] Computer workstation used by authors: "Intel(R) Xeon(R) CPU E5–1650 v4 @ 3.60GHz." 2020.

[28] A. Jagannathan and E.L. Miller, "Three-dimensional surface mesh segmentation using curvedness-based region growing approach," *IEEE Trans. Pattern Anal. Mach. Intell.*, vol. 29, no. 12, pp. 2195–2204, 2007, doi: 10.1109/TPAMI.2007.1125.